Differences in Self-Recognition between Secreted Antibody and Membrane-Bound B Cell Antigen Receptor

Joseena Iype,*,[1] Moumita Datta,*,[1] Ahmad Khadour,*,[1] Rudolf Übelhart,*,[2] Antonella Nicolò,* Tim Rollenske,† Marcus Dühren-von Minden,* Hedda Wardemann,† Palash C. Maity,* and Hassan Jumaa*

The random gene segment rearrangement during B cell development ensures Ab repertoire diversity. Because this process might generate autoreactive specificities, it has been proposed that stringent selection mechanisms prevent the development of autoreactive B cells. However, conventional assays to identify autoreactive B cells usually employ in vitro–generated Abs, which differ from membrane-bound BCRs. In this study, we used a cell-based assay to investigate the autoreactivity of membrane-bound BCRs derived from different B cell developmental stages of human peripheral blood. Contrasted to soluble Ab counterparts, only a few of the tested BCRs were autoreactive, although the cell-based assay sensitively detects feeble Ag recognition of a germline-reverted murine BCR that was selected after OVA immunization of mice, whereas conventional assays failed to do so. Together, these data suggest that proper identification of autoreactive B cells requires the membrane-bound BCR, as the soluble Ab may largely differ from its BCR counterpart in Ag binding. ***The Journal of Immunology*****, 2019, 202: 1417–1427.**

The membrane-bound form of Igs function as a BCR controlling maturation, activation, and differentiation of B cells, whereas the soluble secreted Igs, also known as Abs, contribute to the body's immune surveillance mechanism through pathogen recognition and organization of immune reactions. Ig isotypes IgM, IgD, IgG, IgA, and IgE differ in their C region, and soluble Igs that bind to self-structures are referred to as autoreactive Abs that may induce aberrant immune responses and tissue damage (1–3). Therefore, it has been proposed that developing B cells are subject to rigorous selection during maturation to avoid the development of autoreactive B cells. Indeed, it has been observed that 75% of newly generated immature B cells express autoreactive BCRs (4), and that B cells carrying autoreactive BCRs either modify BCR specificity by receptor editing or are eliminated at early checkpoints of development (5–8). However, a considerable proportion of normal peripheral B cells in healthy individuals express autoreactive Igs, suggesting that additional investigations are required for better understanding of the mechanisms regulating self-recognition and the development of autoimmune diseases.

Conventionally, Ig reactivities are determined by ELISA, surface plasmon resonance (SPR) spectroscopy, or immunofluorescence assay (IFA) on the Hep-2 cell line (4, 9–11) using polyclonal sera or rmAbs. For rAbs, the variable Ig regions cloned from B cells expressing IgM-BCR are expressed as soluble IgG and tested in combination with various autoantigens such as DNA, lipids, insulin, or cell lysates. Based on these results, respective B cells are then classified by IgG/autoantigen interaction as tolerant, autoreactive, or polyreactive (4). ELISA and SPR spectroscopy are standard methods for testing the relative binding, affinity, and avidity of autoantibodies. Because the experimental setup of these assays differs significantly from the membrane-bound BCR situation, these methods are unable to predict Ag binding or the resulting downstream signaling of the respective BCR. Furthermore, depending on the C region or Ig isotype, Abs in their soluble form might have altered Ag-binding properties by modulating specificity or affinity (12, 13). Thus, IgM- and IgD-BCR isotypes expressed on immature or mature (m) B cells may have a different Ag-binding profile than the respective IgG Ab isotype, which is usually expressed in the memory B cell compartment upon class switching. Moreover, different BCR isotypes (e.g., IgM and IgD on m B cells) differ in

*Institute of Immunology, Ulm University Medical Center, 89081 Ulm, Germany; and †Division of B Cell Immunology, German Cancer Research Center, 69120 Heidelberg, Germany

[1]J.I., M.D., and A.K. contributed equally.

[2]Current address: Medical Oncology, National Center for Tumor Diseases, Heidelberg, Germany.

ORCIDs: 0000-0002-9508-9823 (A.K.); 0000-0003-3105-7571 (A.N.); 0000-0003-3921-5933 (H.W.); 0000-0003-3295-5859 (P.C.M.); 0000-0003-3383-141X (H.J.).

Received for publication May 16, 2018. Accepted for publication December 20, 2018.

This work was supported by the Deutsche Forschungsgemeinschaft through IRTG-TRR130: B Cells and Beyond, TRR-130 Project P01, SFB1074, EXC294, and European Research Council Advanced Grant 694992 to H.J. M.D. was supported by European Research Council Advanced Grant 694992. J.I. was supported by a Ph.D. fellowship from the Excellence Initiative of the Deutsche Forschungsgemeinschaft (GSC-4, Spemann Graduate School of Biology and Medicine).

J.I., M.D., A.K., R.U., A.N., and M.D.-v.M. performed the experiments. J.I. and M.D. analyzed data, prepared the figures together with P.C.M., and contributed to the writing of manuscript. M.D., A.N., and P.C.M. prepared revised manuscript. Abs derived from human B cell subsets and anti-OVA Abs were contributed by R.U., T.R., and H.W. H.J. and P.C.M. designed and supervised the entire study and wrote the manuscript. All coauthors discussed the manuscript.

Address correspondence and reprint requests to Dr. Hassan Jumaa, Institute of Immunology, Ulm University Medical Center, Albert-Einstein-Allee 11, 89081 Ulm, Germany. E-mail address: hassan.jumaa@uni-ulm.de

The online version of this article contains supplemental material.

Abbreviations used in this article: B1, B1-like B cell; CBA, cell-based assay; CLL, chronic lymphocytic leukemia; cOVA, cross-linked OVA complex; EV, empty vector; GC, germinal center; HC, H chain; HEL, hen egg lysozyme; IFA, immunofluorescence assay; LC, L chain; m, mature; M-CLL, mutated CLL; MDA, malondialdehyde; mm, IgM^+ memory B cell; ne, new emigrant; OHT, hydroxy tamoxifen; OxdLDL, oxidized low-density lipoprotein; PC-BSA, phosphorylcholine-conjugated BSA; RT, room temperature; Sm, Smith Ag; SPR, surface plasmon resonance; TKO, triple knockout; UM-CLL, unmutated CLL.

their membrane localization and signaling capacities (14, 15). Therefore, it might be misleading to conclude from in vitro Ag binding of soluble IgG that the corresponding IgM-BCR binds to and is activated by the same Ag.

In this study, we used a cell-based assay (CBA) to investigate the differences between IgM-BCR and soluble IgG as well as IgG-BCR in Ag binding and signaling upon the encounter of model Ag, including self-structures (dsDNA). Our data reveal that Ag binding of several Abs expressed as soluble IgG differ dramatically from their IgM-BCR counterpart.

Materials and Methods

Mice and immunization

Female C57BL/6 mice (age: 10–14 wk) were purchased from Charles River Laboratories. Mice were immunized s.c. at the tail base with 100 μg of OVA (Calbiochem) as an alum precipitate in 100 μl of PBS. Mice were sacrificed 21 d postimmunization. Animal experiments were approved by the local authority.

Isolation of mAb GC178 and human B1-like B cell–derived Abs

Single cell sorting, RT-PCR, Ig gene cloning, and mAb generation of germinal center (GC) B cells (7-AAD$^-$B220$^+$Fas$^+$GL7$^+$IgD$^-$) from lymph nodes were performed as previously described (16). Briefly, cDNA from single GC B cells was synthesized by reverse transcription, and Ig genes were amplified using a seminested PCR approach and sequenced. For human B1-like B cell (B1)–derived Abs, CD20$^+$CD27$^+$CD43$^+$CD70$^-$CD5$^+$ B1 cells were purified by sorting from the peripheral blood of a healthy human donor and Ig genes were amplified and cloned as previously described (4, 17).

Ig gene reversion of GC178 to the unmutated germline form

Reversion of GC178 was performed using a PCR-based strategy as previously described (17). Briefly, the unmutated V gene was amplified using primers specific for the V gene leader sequence and primer located at the 3′ end of the framework region 3. The CDR3 junction of the GC178 Ig gene was amplified by PCR using an overlapping the primer at the 3′ end of framework region 3 and a J gene–specific primer. The unmutated V gene and the CDR3-J segment were fused by overlapping PCR, and successful reversion was confirmed by sequencing.

Cell culture

Phoenix and triple knockout (TKO) cells were cultured in Iscove medium (Biochrom) containing 10% FCS (PAN-Biotech), 10 mM L-glutamine (Life Technologies), and 100 U/ml each of penicillin and streptomycin (Life Technologies). For TKO cells, the medium was supplemented with 50 mM 2-ME (Life Technologies) and murine IL-7–enriched medium obtained from J558L mouse plasmacytoma cells stably transfected with a murine IL-7 expression vector.

Plasmids and retroviral transduction

Ig H chain (HC) and L chain (LC) were expressed using the BiFC vector system described previously (18). To generate GC178 and GC178 IgM-BCRs, Ig VH and VL genes were cloned into murine Igμ and murine Igκ expression vectors. BCRs derived from different single B1, new emigrant (ne), m, IgM$^+$ memory B cells (mm), and chronic lymphocytic leukemia (CLL) B cells were amplified by an anchor PCR using poly(G)–tailed cDNA and a poly(C)–containing primer as described before (4, 19, 20). For their expression in TKO cells, vectors encoding the complete human LCs were used, whereas the human VH domains were cloned into the murine Igμ or human Igγ1 and Igμ constant domains. Retroviral transduction was performed as described previously (18, 21). Briefly, phoenix cells were transfected using GeneJuice (Novagen) as recommended by the manufacturers protocol. Supernatants were harvested 48 h posttransfection and used for transduction of TKO cells.

Flow cytometry

To analyze BCRs expressing TKO cells and to identify mouse and human B cell subsets, the following fluorescently labeled Abs were used: anti-mouse IgM eFluor 450 (eb121-15F9; eBioscience), anti-mouse IgM Cy5 (polyclonal; Jackson ImmunoResearch), biotin labeled anti-human κ or λ (polyclonal; SouthernBiotech), anti-mouse IgM allophycocyanin (RMM-1; BioLegend), Alexa Fluor 647–conjugated anti-human IgM (MHM-88; BioLegend), anti-human IgG (polyclonal; SouthernBiotech), anti-human CD20 allophycocyanin (2H7; BioLegend), anti-human CD27 V450 (M-T271; BD Biosciences), anti-human CD43 FITC (eBio84-3C1; eBioscience), anti-human CD70 PE (Ki-24; BD Biosciences), and anti-human CD5 PE–Cy7 (UCHT2; BioLegend).

Biotinylation of dsDNA

One microgram of calf thymus DNA was fragmented by digesting with a mixture of blunt end cutter restriction enzymes (SmaI, HincII, and EcoRV) and purified with a gel extraction column (QIAGEN). Klenow fragment (New England Biolabs)–mediated biotin labeling reaction was performed with 100 μM random hexamer and a mixture of unlabeled dNTPs (0.1 mM each of dATP, dGTP, dCTP, and 0.04 mM dTTP) and Biotin-11-dUTP (0.06 mM). Afterwards biotinylated DNA was again column purified.

Ag-binding assay

For Ag binding, TKO cells expressing the BCR of interest were incubated with biotinylated Ags at 20 μg/ml oxidized low-density lipoprotein (OxdLDL) (MyBioSource), 10 μg/ml LPS (Invivogen), 20 μg/ml phosphorylcholine-conjugated BSA (PC-BSA) (Biosearch Technologies), 20 μg/ml malondialdehyde (MDA)-BSA (Academy Bio-Medical), 20 μg/ml MDA-LDL (Cell Biolabs), 20 μg/ml Smith Ag (Sm) (AROTEC Diagnostics), and different doses of dsDNA from calf thymus (Invitrogen), OVA (Sigma-Aldrich), and hen egg lysozyme (HEL; Sigma-Aldrich) for 20 min on ice. After washing, Ag binding was detected by allophycocyanin-conjugated streptavidin (eBioscience). The cells were costained with fluorescently labeled HC Ab and anti-mouse IgM eFluor 450 (eBioscience) and analyzed in a BD LSRFortessa I (BD Biosciences) and analyzed using FlowJo software (TreeStar).

Measurement of Ca^{2+} flux

Ca^{2+} analyses were performed as described (18, 21). Briefly, a total of 1×10^6 freshly transduced TKO cells expressing ERT2-SLP65 were loaded with Indo-1 AM (Invitrogen) using Pluronic F27 (Invitrogen). ERT2-SLP65 function was induced by the addition of 1–2 μM 4-hydroxy tamoxifen

Table I. Abs expressed as IgM and IgG1 for testing their responsiveness toward dsDNA

Specificity/Ab Name	Cloned from	Original Isotype	Origin Species	Expressed in TKO as
B1-9	B1	IgM	Human	B1-9 IgM and IgG1
m-GO53	m naive	IgM	Human	m-GO53 IgM and IgG1
UM-CLL2	CLL patient	IgM	Human	UM-CLL2 IgM and IgG1
2C6	Commercially available anti-OVA	IgE	Mouse	OVA IgM and IgG1
HEL	HEL-specific BCR	IgM	Mouse	HEL IgM and IgG1
m-GO43	m naive	IgM	Human	m-GO43 IgM and IgG1
m-GO16	m naive	IgM	Human	m-GO16 IgM and IgG1
m-JH.2A8	m naive	IgM	Human	m-JH.2A8 IgM and IgG1
B1-36	B1	IgM	Human	B1-36 IgM and IgG1
mm-GO9	m memory	IgM	Human	mm-GO9 IgM and IgG1
mm-GO30	m memory	IgM	Human	mm-GO30 IgM and IgG1
ne-GO18	ne	IgM	Human	ne-GO18 IgM and IgG1
ne-GO77	ne	IgM	Human	ne-GO77 IgM and IgG1

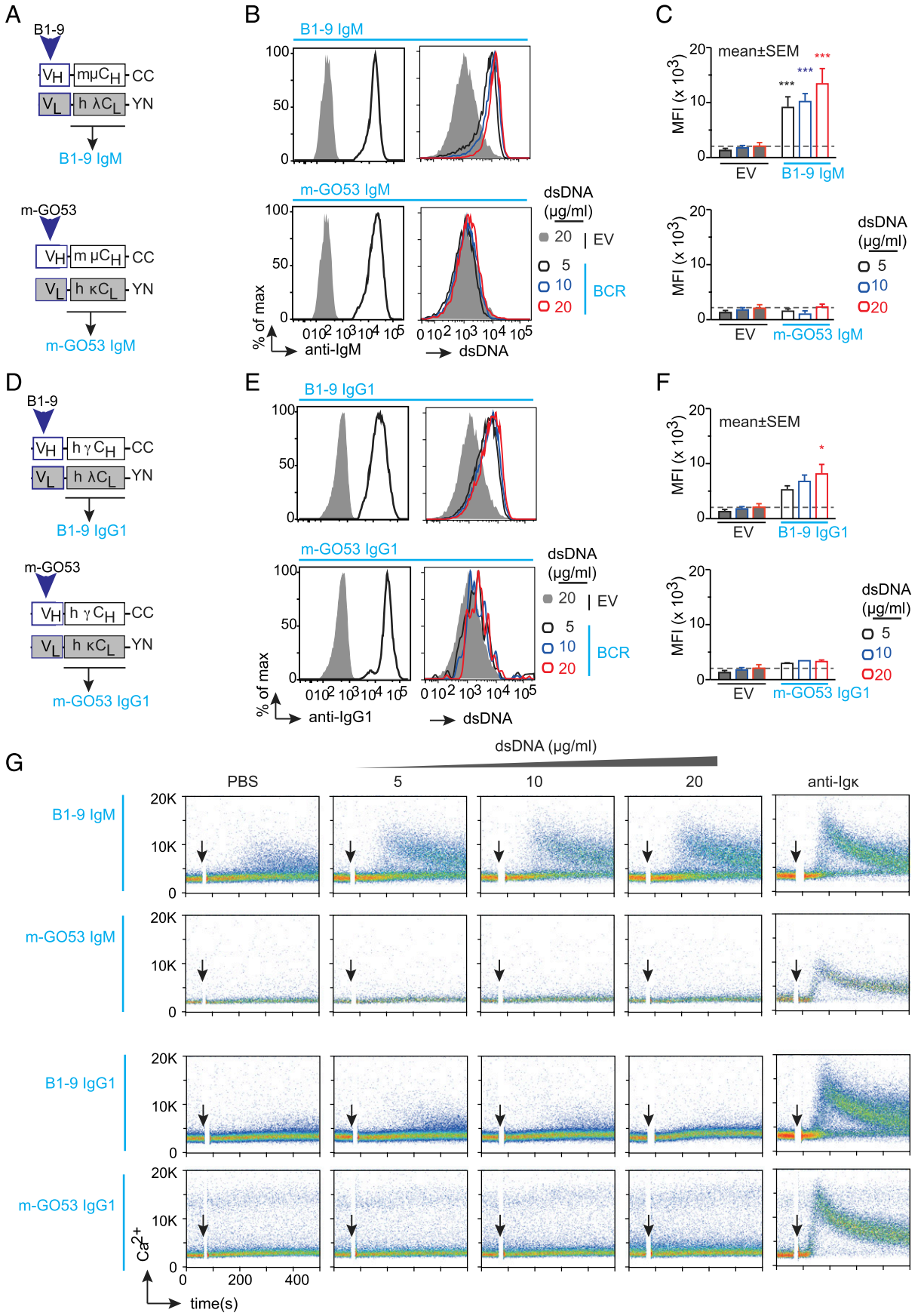

FIGURE 1. Differential response of IgM and IgG-BCR isotypes toward dsDNA. (**A**) Schematic representation of plasmids encoding Ig HC and LC of B1-9 (top) and m-GO53 (bottom) cloned as murine IgM-BCRs. (**B**) Left, Representative analysis of BCR expression determined by surface IgM staining followed by FACS of B1-9 IgM (top) and m-GO53 IgM (bottom) expressing TKO cells compared with the EV control. Right, Representative histograms showing dsDNA binding at different dsDNA concentration by B1-9 IgM (top) and m-GO53 IgM (bottom) expressing *(Figure legend continues)*

(OHT) (Sigma-Aldrich). For BCR stimulation, calf thymus DNA, OVA, cross-linked OVA complexes (cOVA), and HEL at different concentrations (as detailed in the figure legends) and anti-human or anti-murine Ig LC (Igκ or Igλ) Ab at 10 μg/ml (SouthernBiotech) were used.

Biotinylation of Ags

The Ags were biotinylated using FluoReporter Mini-biotin-XX Protein Labeling Kit (Invitrogen). In brief, 1 mg of target Ag was incubated with 0.1 mg biotinamidohexanoic acid N-hydroxysuccinimide ester (Sigma-Aldrich) at room temperature (RT) for 1 h. The reaction mixture was then dialyzed against PBS at 4°C.

Cross-linking of OVA

To cross-link OVA, biotinylated OVA was mixed with unconjugated streptavidin (Life Technologies) or allophycocyanin-conjugated streptavidin (eBioscience) in a molar ratio of 2:1 and incubated on ice for 20 min.

rAb production and purification

Abs were produced in vitro as described previously (4, 17). In brief, human embryonic kidney fibroblast 293A cells were cotransfected with 15 μg/ml Ig HC– and Ig LC–encoding plasmids by calcium phosphate precipitation. Cells were washed with serum-free cell DMEM (Invitrogen) 8–12 h posttransfection and thereafter cultured in DMEM supplemented with 1% Nutridoma-SP (Roche). Supernatants were harvested after 8 d and purified using protein G–Sepharose (GE Healthcare) and eluted with 0.1 M glycine (pH 3). The pH of the elute was neutralized with 1 M Tris (pH 8) supplemented with 0.05% sodium azide. Concentrations of the purified Abs were determined by anti-human IgG ELISA using human monoclonal IgG1 (Jackson ImmunoResearch) as standard.

ELISA and IFA

ELISA were performed as described previously (4). Briefly, microtiter plates (Costar) were coated with individual Ags at 10 μg/ml for dsDNA and LPS (Sigma-Aldrich), 5 μg/ml for recombinant human insulin (Sigma-Aldrich), and 10 μg/ml for OVA (Sigma-Aldrich). Purified Abs were adjusted to 1 μg/ml and used at three serial dilutions of 1:4 in PBS, and Abs were detected with HRP-labeled goat anti-human IgG (Jackson ImmunoResearch). IFAs were done as previously described (4). Briefly, Hep-2 Ag substrate–coated slides (MBL Bion) were incubated at RT with 15 μl of purified Abs (1 mg/ml). After washing, Cy3-conjugated anti-human IgG1 Ab (Jackson ImmunoResearch) was used to detect binding, and nuclear staining was performed using DAPI.

SPR spectroscopy

Affinity measurements were performed on a Biacore T200 (GE Healthcare). A CM5 chip (GE Healthcare) was coupled with mouse anti-human IgG (GE Healthcare), according to the manufacturer's instructions. Measurements and dilutions were performed in PBS containing 0.05% Tween 20. All steps were performed at RT. rmAbs diluted to 25 μg/ml were immobilized for 60 s at a flow rate of 10 μl/min followed by a stabilization period of 120 s. OVA (Calbiochem) was floated for 60 s at a flow rate of 30 μl/min over the chip surface and allowed to dissociate for 180 s. Flow rate was maintained, and the chip surface was regenerated by injection of 3 M MgCl2 for 30 s. Ag binding is depicted as the difference in resonance units between sample and reference flow cell. Affinity was calculated using the 1:1 binding model of the Biacore T200 software V2.0.

Cell-based ELISA

Ninety-six–well glass-bottom and black-walled plates (μ-Plate 96 well; IBIDI) were coated with 100 μl 0.5 μg/ml fibronectin in PBS for 30 min at RT. After washing, cells were added at a density of 250,000 cells per well and were kept on ice for 15 min to adhere to the surface. Afterwards, empty plate surfaces were blocked with 3% BSA in PBS followed by addition of biotinylated DNA at 0.25 μg/ml concentration for 15 min on ice. Cells were then washed with PBS and incubated with diluted (1:8000) HRP-conjugated streptavidin (Thermo Scientific Scientific) for 15 min on ice. After washing, DNA binding was detected by colorimetric assay using TNB substrates (Biozol) by measuring the color at 450 nm.

Statistical analysis

Statistical analyses were performed using GraphPad Prism 6 software (GraphPad). Specific tests of statistical significance are detailed in the figure legends.

Results

Differential response of IgM- and IgG-BCR isotypes toward autoantigen (dsDNA)

There is an increasing body of evidence demonstrating that the Ig isotypes influence the specificity and affinity of soluble Abs (12, 13, 22) as well as BCRs (15). Therefore, we first examined and compared the reactivity of different IgM- and IgG-BCR isotypes (Table I). We analyzed BCRs derived from a polyreactive Ab, named as B1-9, which we cloned from human B1 (Fig. 1A, 1D). As a control, we used BCR isotypes derived from the m-GO53 Ab that was previously cloned from a human peripheral m B cell (4) (Fig. 1A, 1D). We used the TKO cells, derived from a RAG2, λ5, and SLP65 TKO mice (21) to reconstitute BCR expression (Fig. 1B, 1E, left panels). Next, we analyzed the binding of these BCRs to different concentrations of dsDNA (5, 10, and 20 μg/ml). Both B1-9 IgM and B1-9 IgG1 bind to different doses of dsDNA, whereas the m-GO53 IgM and IgG1 failed to bind (Fig. 1B, 1E, right panels). Of note, B1-9 IgM binds more than B1-9 IgG1 (Fig. 1C, 1F). Next, we analyzed the signaling capacity of these receptors by measuring intracellular Ca^{2+} release in response to the aforementioned doses of dsDNA. Interestingly, B1-9 IgM-BCR showed Ca^{2+} release in response to all doses of dsDNA, whereas B1-9 IgG1-BCR showed no Ca^{2+} release in TKO cells (Fig. 1G). Thus, despite binding to dsDNA at all doses (Fig. 1E, 1F), B1-9 IgG1 BCR failed to mobilize Ca^{2+} (Fig. 1G). Moreover, B1-9 IgM but not B1-9 IgG1 showed a cell-autonomous Ca^{2+} release (15, 18, 20) upon inducible activation of SLP65 by addition of 4-OHT in absence of any dsDNA (Fig. 1G). This result suggests that B1-9 IgM is autonomously active BCR and elicits Ca^{2+} mobilization, most likely because of polyreactivity (18). As expected, no BCR activation after dsDNA treatment was observed in cells expressing the control m-GO53 as IgM or IgG1 (Fig. 1G). Similar results were obtained for all B1-9 IgM-BCRs regardless whether human or murine IgM C regions were used (Supplemental Fig. 1A–D).

To substantiate our findings from flow cytometric analysis, we developed another cell-based ELISA to measure relative DNA binding by these receptors (Supplemental Fig. 1E).

TKO cells compared with the EV. (**C**) Quantification of relative dsDNA binding by B1-9 IgM (top) and m-GO53 IgM (bottom) expressing TKO cells compared with the EV. Bars represent mean ± SEM. (**D**) Same as in (A) for B1-9 (top) and m-GO53 (bottom) cloned as human IgG1 BCRs. (**E**) Left, Same BCR expression analysis as in (B) for B1-9 IgG1 (top panels) and m-GO53 IgG1 (bottom panels) expressing TKO cells compared with the EV control. Right, Similar dsDNA-binding analysis as in (B) for B1-9 IgG1 (top panels) and m-GO53 IgG1 (bottom panels) expressing TKO cells. (**F**) Similar quantification as in (C) of relative dsDNA binding by B1-9 IgG1 (top) and m-GO53 IgG1 (bottom) expressing TKO cells compared with the EV. (C) and (F) were analyzed by two-way ANOVA, Dunnett multiple comparison test. $*p < 0.05$, $***p < 0.001$. (**G**) Representative calcium release of B1-9 IgM, m-GO53 IgM, B1-9 IgG1, and m-GO53 IgG1 expressing TKO cells in response to control PBS or indicated concentrations of dsDNA and 10 μg/ml of anti-LC (κ or λ). Of note, in each calcium experiment, cells received 2 μM 4-OHT along with the stimuli to induce ERT2-SLP65 activity. The data in (B), (C), and (E)–(G) are representative of three independent experiments.

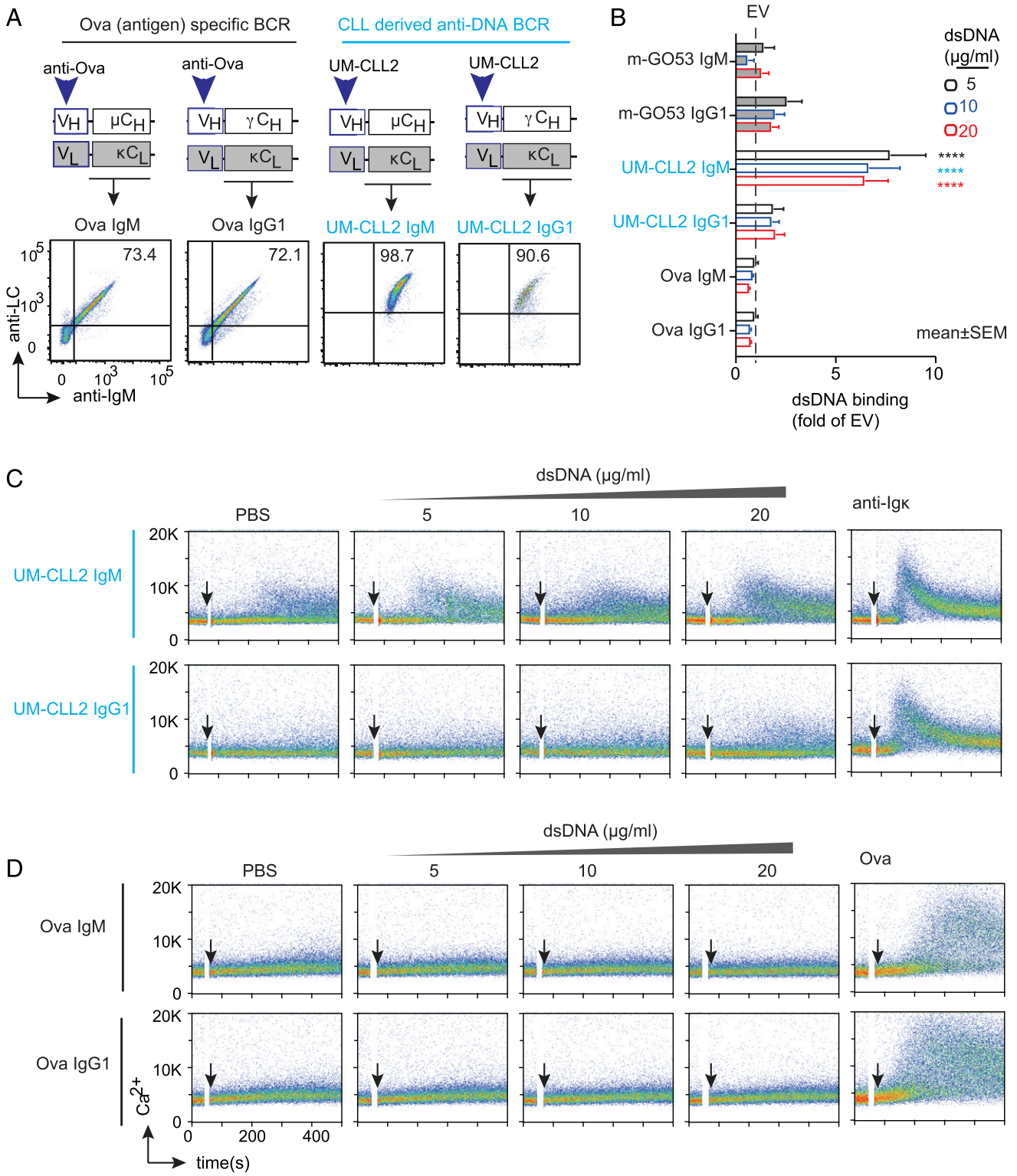

FIGURE 2. dsDNA binding by autoreactive UM-CLL2 BCRs and HEL-specific BCRs. (**A**) Top panel, Schematic representation of plasmids encoding HC and LC of anti-OVA and UM-CLL2 cloned as murine IgM and human IgG1 BCRs. Bottom panel, Representative FACS analysis of BCR expression. (**B**). Quantification of dsDNA binding by UM-CLL2 IgM, UM-CLL2 IgG1, OVA IgM, and OVA IgG- expressing TKO cells compared with mGO53 IgM and IgG1 expressing cells. The relative binding of EV is indicated with the dashed line. Bars represent mean ± SEM. ****$p < 0.0001$, two-way ANOVA, Dunnett multiple comparison test. (**C** and **D**) Representative Ca^{2+} release of UM-CLL2 IgM and UM-CLL2 IgG1 (C) and OVA IgM and OVA IgG1 (D) expressing TKO cells in response to control PBS or indicated concentrations of dsDNA, 10 μg/ml of anti-LC (κ or λ), and 10 μg/ml of soluble OVA. In each calcium experiment, cells received 2 μM 4-OHT along with the stimuli to induce ERT2-SLP65 activity. Data in (B)–(D) correspond to three independent experiments.

To this end, we seeded TKO cells expressing different receptors of interest in a fibronectin-coated 96-well glass-bottom plate and incubated them with biotinylated dsDNA (Supplemental Fig. 1E). Bound DNA was quantified by colorimetric assay using HRP-labeled streptavidin. Similar to flow cytometric data, B1-9 IgM and B1-9 IgG1 expressing TKO cells manifested significantly

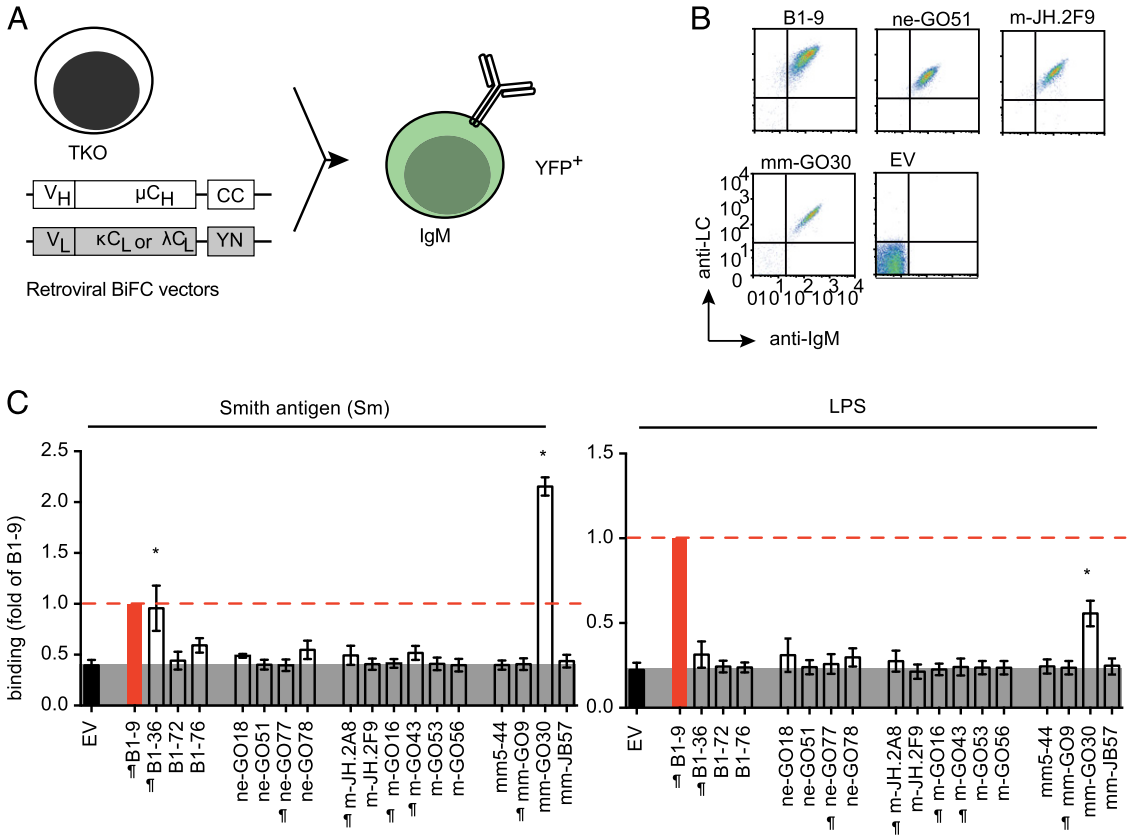

FIGURE 3. Autoantigen-binding profile of BCRs from different peripheral B cells subsets. (**A**) Schematic representation of TKO cell reconstitution with retroviral constructs encoding HC and LC derived from different human B cell subsets expressed as murine IgM in TKO cells. (**B**) Representative FACS analysis of BCR expression. The BCRs derived from different B cell subsets were indicated by their subset identifiers: B1, ne, naive m, and mm, followed by clone numbers. The dot plot represents Ig HC and Ig LC expression measured using anti-murine IgM and anti-human LC (κ or λ) polyclonal Abs and compared with the EV control. (**C**) Quantification of Sm (left panel) and LPS (right panel) binding to IgM-BCRs derived from different human B cell subsets in TKO cells. The bar graph represents mean ± SEM Ag binding to different IgM-BCRs in TKO cells measured by fold change in median fluorescence intensity (MFI) of transduced (YFP^+) and untransduced cells (YFP^-) and compared by using unpaired, nonparametric Mann–Whitney *U* test. $*p < 0.05$. Data are normalized to B1-9 IgM expression (solid red bar) and the normalization value is indicated by a red dashed line. The gray shaded area represents background signal in EV control. BCRs denoted with the ¶ symbol were previously described (4, 23) to exhibit polyreactivity, and unlabeled BCRs were nonpolyreactive as soluble IgG Abs in ELISA. The data in (B) and (C) correspond to a minimum of three independent experiments.

higher DNA binding compared with mGO53 IgM and IgG1 or empty vector (EV)-expressing cells (Supplemental Fig. 1E, 1G). We also tested the ability of DNA binding by the secreted B1-9 IgM, B1-9 IgG1, and mGO53 IgM Abs using traditional ELISA (Supplemental Fig. 1F). We found that both B1-9 IgM and IgG1 have significantly higher DNA-binding ability compared with mGO53 IgM (Supplemental Fig. 1F). Importantly, DNA-binding ability of B1-9 IgM Ab was shown to be higher than that of B1-9 IgG1, as has also been observed in their receptor form in the flow cytometric assay (Fig. 1C, 1F).

The above data suggest that B1-9 elicited Ca^{2+} response to dsDNA only when expressed as IgM but not as IgG1-BCR (Fig. 1G). To validate this differential response of IgM and IgG1 in another autoreactive BCR, we used a CLL-derived receptor namely, unmutated CLL (UM-CLL) 2, and also OVA-specific BCR as a control (Fig. 2A, upper panels). In TKO cells, both UM-CLL2 and OVA-specific BCR were successfully expressed either as surface IgM or IgG1 (Fig. 2A, lower panels). When tested for dsDNA binding, UM-CLL2 IgM-expressing cells showed significantly higher DNA binding compared with m-GO53 IgM and m-GO53 IgG1, whereas UM-CLL2 IgG1 or OVA IgM- and IgG1-expressing cells showed negligible binding (Fig. 2B). Next, when these cells were tested for Ca^{2+} release in response to DNA binding, only UM-CLL2 IgM elicited Ca^{2+} flux (Fig. 2C, 2D). In addition to the OVA-specific BCR, we also used HEL Ag-specific BCR in IgM and IgG1 forms as further control (Supplemental Fig. 2A). Similar to OVA IgM and OVA IgG1, HEL IgM and HEL IgG1 showed no dsDNA binding (Supplemental Fig. 2B) and subsequent Ca^{2+} mobilization (Supplemental Fig. 2C). Taken together, these data demonstrate unexpected differences in autoantigen binding and signaling capacity of the IgM-BCR isotype as compared with class-switched IgG.

Autoantigen-binding profile of BCRs from different peripheral B cell subsets

The frequency of autoreactive Ig specificities is predominant in the bone marrow compartment as demonstrated by several rIgG Abs cloned from different human B cell subsets corresponding to ne, peripheral B1, m naive or mm (4, 23). However, these B cell subsets express membrane-bound IgM-BCRs during their development. Hence, it is essential to analyze the autoreactive specificities in the distinct B cell subsets as membrane bound IgM-BCRs. To address whether these Abs are auto/polyreactive as membrane-bound IgM, we expressed the aforementioned Abs as membrane-bound IgM-BCR (Fig. 3A,

Table II. List of Abs derived from different B cell subsets and their binding to different Ags

Origin B Cell Subset	FACS Phenotype	Name of Ig	LC	As IgM-BCR		As IgG Ab				Reference
				Sm	LPS	dsDNA	LPS	Insulin	Hep-2	
B1	$CD19^+CD20^+$	B1-9	λ	+	+	+	+	+	+	Described in this article
	$CD27^+CD43^+$	B1-36	κ	+	−	+	+	+	+	Described in this article
	$CD70^-$	B1-72	λ	−	−	−	−	−	+	Described in this article
		B1-76	κ	−	−	−	−	−	+	Described in this article
ne	$CD19^+CD10^+$	ne-GO18	λ	−	−	−	−	−	−	Wardemann et al., 2003 (4)
	IgM^+CD27^-	ne-GO51	κ	−	−	−	−	−	+	Wardemann et al., 2003 (4)
		ne-GO77	κ	−	−	+	+	+	+	Wardemann et al., 2003 (4)
		ne-GO78	κ	−	−	−	−	−	−	Wardemann et al., 2003 (4)
m naive	$CD19^+CD10^-$	m-JH.2A8	κ	−	−	+	+	+	+	Wardemann et al., 2003 (4)
	IgM^+CD27^-	m-JH.2F9	κ	−	−	−	−		−	Wardemann et al., 2003 (4)
		m-GO16	κ	−	−	+	+	+	−	Wardemann et al., 2003 (4)
		m-GO43	κ	−	−	−	−	−	+	Wardemann et al., 2003 (4)
		m-GO53	κ	−	−	−	−	−	−	Wardemann et al., 2003 (4)
		m-GO56	κ	−	−	−	−	−	−	Wardemann et al., 2003 (4)
IgM^+ memory	$CD19^+CD10^-$	mm5-GO44	λ	−	−	−	−	−	−	Tsuiji et al., 2006 (23)
	IgM^+CD27^+	mm-GO9	λ	−	−	+	+	+	−	Tsuiji et al., 2006 (23)
		mm-GO30	κ	+	+	−	−	−	−	Tsuiji et al., 2006 (23)
		mm-JB57	κ	−	−	−	−	−	−	Tsuiji et al., 2006 (23)

+ and − represent positive and negative for Ag binding, respectively.

Table II) and used our CBA to test their binding to a common autoantigen referred to as Sm or to LPS as foreign Ag. All BCRs were expressed on TKO cells (Fig. 3B, Supplemental Fig. 3A) and showed signaling activity in response to anti-BCR treatment.

We found that the majority of polyreactive soluble Igs lacks autoreactivity when expressed as membrane-bound IgM (Fig. 3C, Supplemental Fig. 3B, Table II). For instance, although rIgG1 Abs derived from ne-GO77 or from m naive B cells (m-JH.2A8 and m-GO16) bind to LPS when expressed as soluble Ig in vitro (4); binding to LPS was not detected when these Igs were expressed as IgM-BCRs in CBA (Fig. 3C and Table II). Similarly, among four BCRs derived from mm, only mm-GO30 showed binding to LPS and Sm (Fig. 3C), which was not previously detected when expressed as soluble IgG1 in vitro (23). Of note, the binding capacities of peripheral B1 cell–derived Abs were not previously analyzed (4, 23). Therefore, these Igs were expressed as soluble IgG1 to perform the conventional tests and evaluate the binding of these Abs to DNA, LPS, and insulin in ELISA (Supplemental Fig. 3C) and in IFA on Hep-2 cells (Supplemental Fig. 3D). The B1-9–derived soluble IgG1 showed highest binding to dsDNA, LPS, and insulin (Fig. 3C, Supplemental Fig. 3D). Soluble B1-36 showed weak polyreactivity when expressed as soluble IgG1 but bound to both Sm and LPS as IgM-BCRs in CBA (Fig. 3C, Supplemental Fig. 3C). Taken together, our results show the in vitro binding of rIgG markedly differ from the IgM-BCR counterpart. To further confirm our observation, we cloned these aforementioned BCRs as human IgM and human IgG1 isotypes and expressed them in TKO cells (Supplemental Fig. 3E, 3F, Table I). When tested for dsDNA binding, ne-GO77, mm-GO30, and B1-36 receptors were found to bind dsDNA only in IgM form, whereas none of them binds to dsDNA in IgG1 form (Supplemental Fig. 3E, 3F). It is, therefore, conceivable that being expressed as IgM is not the reason why the CBA did not confirm the autoreactivity of previously described Igs tested as soluble IgG1 (4, 10, 23). No reactivity was detected even when these BCRs were expressed as membrane-bound IgG1 form. Thus, the autoreactivity of soluble IgG1 seems not to correspond to the reactivity of its membrane-bound BCR form. Because the BCR format is physiologically relevant for selection of developing B cells prior to differentiation into plasma cells, our data suggest that these differences need to be considered when Ig genes from different B cell subsets are cloned and subsequently used to produce soluble Abs to conclude the Ag-binding profile of the respective B cells.

Ag-binding profile of CLL-derived BCRs

Because binding to an autoantigen has been proposed to be the underlying mechanism for BCR-mediated activation and proliferation of B cell neoplasms, including CLL, we investigated the Ag-binding profile of CLL-derived Igs when expressed as BCR. Notably, previous studies mainly analyzed recombinant soluble IgG Abs cloned from CLL B cells and found that a substantial fraction of CLL B cells from UM-CLL or mutated CLL (M-CLL) cases show increased autoreactivity when tested in conventional readouts (9), suggesting that the respective BCRs are autoreactive. To test this in the CBA, we analyzed 10 M-CLL and 5 UM-CLL IgM-BCRs (Fig. 4A, 4B, 4D) for their binding to several autoantigens (24–26), including Sm, PC-BSA, OxdLDL, MDA-BSA, MDA-LDL, and LPS. Compared with the EV, all M-CLL–derived IgM-BCRs and UM-CLL–derived IgM-BCRs were expressed on TKO cells (Fig. 4B and data not shown). We used B1-9 IgM (Fig. 4C) and m-GO53 IgM as positive and negative control, respectively. Surprisingly, within our analyzed cohort, no significant Ag binding to CLL BCRs was observed (Fig. 4D). Of note, M-CLL3, UM-CLL1, and UM-CLL2 in their soluble IgG1 form were shown to bind Ags like LPS and insulin in ELISA and to be reactive on Hep-2 cells in IFA (20). These data reveal clear differences between soluble IgG and membrane-bound BCR, suggesting that the autoreactive Abs are not always presented as autoreactive BCRs.

Differential OVA binding by soluble IgG Abs and IgM-BCRs

To confirm the strength of the CBA, we evaluated its ability to monitor affinity maturation of an Ab during GC reaction. To this end, we used OVA as model Ag for immunization and investigated an Ig that was derived from a single GC-derived B cell recognizing OVA (Fig. 5A). This Ig, designated as GC178,

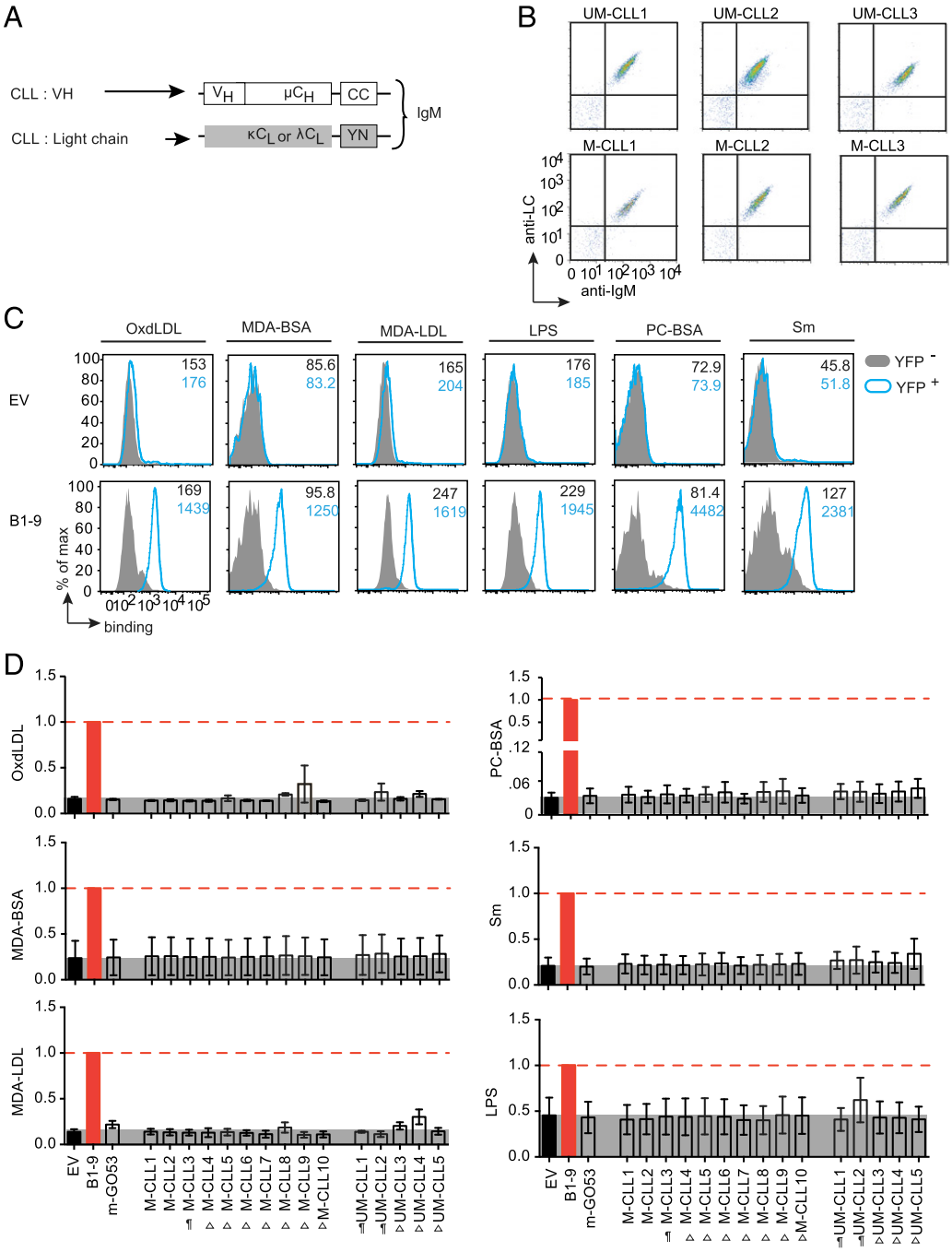

FIGURE 4. Autoantigen-binding profile of CLL-derived BCRs. (**A**) Schematic representation of retroviral constructs encoding HC and LC of BCRs derived from different M-CLL (n = 10) and UM-CLL (n = 5) expressed as murine IgM in TKO cells. (**B**) Representative FACS analysis of BCR expression. The dot plot represents Ig HC and Ig LC expression of six BCRs derived from UM-CLL and M-CLL measured using anti-murine IgM and anti-human LC (κ or λ) polyclonal Abs. The expression data of remaining UM-CLL– and M-CLL–derived BCRs were previously published (20). (**C**) Representative FACS analysis of different Ag binding of B1-9 IgM-BCR compared with EV control. The Ags are OxdLDL, MDA-BSA, MDA-LDL, LPS, PC-BSA, and Sm as summarized in Fig. 3C. The histogram overlays show Ag binding to transduced YFP$^+$ cells (blue) compared with untransduced YFP$^-$ cells (solid gray), and the median fluorescence intensity (MFI) values are indicated in the histogram. The data are representative of a minimum of three independent experiments. (**D**) Quantification of different Ag binding to CLL-derived BCRs as indicated. The bar graph represents mean ± SEM Ag binding to different IgM-BCRs measured by fold change in MFI of YFP$^+$ and YFP$^-$ and compared by using unpaired, nonparametric Mann–Whitney U test. Data are normalized to B1-9 IgM expression (solid red bar), and the normalization value is indicated by a red dashed line. The gray shaded area represents background signal in EV control. The Ags are OxdLDL, MDA-BSA, MDA-LDL, LPS, PC-BSA, and Sm. BCRs derived from CLL cells labeled as "¶" were previously described (20) to exhibit polyreactivity and the unlabeled BCRs were nonpolyreactive as IgG Abs in ELISA. "Δ" denotes the BCRs that were not analyzed for polyreactivity as IgG Abs. The data in (B) and (C) correspond to a minimum of three independent experiments.

was also reverted to germline sequence and named GC178gl (Supplemental Fig. 4A). We analyzed OVA binding of GC178 and GC178gl produced as soluble IgG1 and compared them in ELISA and SPR spectroscopy to a commercially available anti-OVA Ab known as clone 2C6 (Fig. 5B, 5C, Supplemental Fig. 4B). As negative controls, we used IgG1 derived from

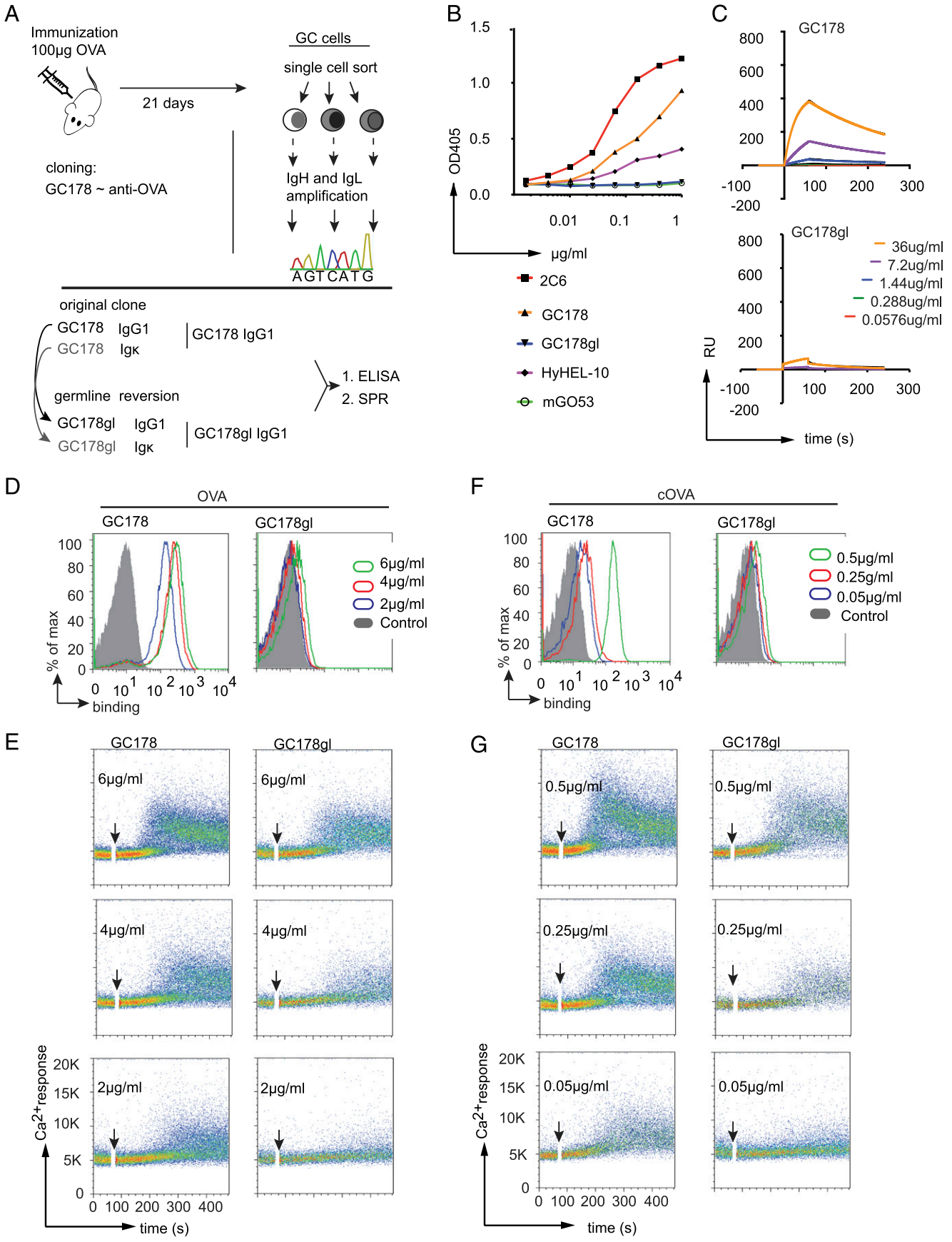

FIGURE 5. Comparison of anti-OVA reactivity of GC178 and GC178gl IgG1 Abs and its membrane-bound BCR forms. (**A**) Schematic depicts cloning of GC-derived anti-OVA Ab named GC178 (top). The Ig HC and Ig LC of GC178 were reverted to their germline sequence (GC178gl), and both of them were produced as IgG1 Ab. (**B**) ELISA analysis of OVA binding of GC178 (orange) and GC178gl (blue) IgG1 Abs in comparison with commercial anti-OVA (2C6, red), anti-HEL Ab (HyHEL10, purple) and negative control (m-GO53, green). (**C**) Representative SPR spectroscopy *(Figure legend continues)*

anti-HEL Ab (HyHEL10) and m-GO53 IgG1. As expected, the GC178 Ab bound to OVA, whereas the germline-reverted GC178gl surprisingly failed to bind OVA in ELISA and showed feeble binding at a very high concentration (36 μg/ml) in SPR (Fig. 5B, 5C). Of note, anti-OVA Ab derived from 2C6 showed the highest binding in both ELISA and SPR (Fig. 5C, Supplemental Fig. 4B).

In contrast, when GC178 and GC178gl Ig were expressed as IgM-BCRs (GC178 IgM and GC178gl IgM), both showed binding to OVA (Fig. 5D). In parallel, we also analyzed the ability of GC178 and GC178gl IgM-BCRs to induce Ca^{2+} flux in response to OVA treatment. Both IgM-BCRs showed an elevated Ca^{2+} response toward different concentrations of OVA (Fig. 5E). Notably, reverting the GC-derived GC178 into its germline counterpart GC178gl was associated with drastic decrease in OVA binding. Nonetheless, the subtle binding of GC178gl IgM-BCR to OVA was enough to trigger Ca^{2+} release (Fig. 5E). Furthermore, we also determined the binding of both GC178 and GC178gl IgM-BCR to OVA presented as complexes. To this end, cOVA were generated by biotinylation and subsequent incubation with streptavidin. Interestingly, both GC178 and GC178gl IgM-BCRs showed increased binding and Ca^{2+} release in response to cOVA (Fig. 5F, 5G). Importantly, both GC178 and GC178gl IgM-BCR showed stronger binding and triggered Ca^{2+} release in response to much lower concentrations of cOVA as compared with soluble OVA (Fig. 5F). The negative control HyHEL10 IgM-BCR showed no binding to the highest concentration (6 μg/ml) of OVA (Supplemental Fig. 4C, 4D).

Discussion

In summary, our data reveal important differences in Ag binding between IgM-BCR and soluble IgG Ab. The main finding is that most Abs that are identified to be autoreactive as soluble Abs in conventional assays are not autoreactive when expressed as membrane-bound IgM on the B cell surface. This suggests that investigating the autoreactivity of B cells requires the employment of cell-based systems, as Ags defined using secreted IgG Abs or Fab fragments may not correspond to IgM-BCR binding.

Importantly, the ability of the CBA to properly monitor Ag binding specifically for low-affinity Ag is demonstrated by the results showing that only CBA but neither ELISA nor SPR detects Ag binding of a GC-derived BCR after reversion to the putative germline sequence to evaluate Ag binding prior to somatic hypermutation. These data underline the sensitivity of the CBA and suggest that the lack of autoreactivity for most of the BCRs tested in this study is not because of lower sensitivity of the cellular system, it is rather an intrinsic property of the receptors. Thus, whereas ELISA and SPR are appropriate methods for testing the relative binding, affinity, and avidity of soluble Abs, they seem not be ideal for determining the Ag spectrum of membrane-associated BCR, which requires a cellular system.

Moreover, the view that the variable domain solely determines Ag specificity seems to be incomplete, as increasing evidence suggests that the C region of the Ab, which induces substantial conformational changes and mutual effects in the variable and constant parts of an Ab, is involved in Ag binding (27). Interestingly, not only the affinity but also the recognized epitopes seem to largely depend on the isotype of the C region (13, 28, 29). In line with this, our results suggest that Ags identified using the V region of BCRs from different B cell subsets may not match the Ags that are recognized by IgM-BCR on the cell surface. In addition, the BCR on the cell surface might be organized in a conformation that regulates its accessibility to Ag, thereby limiting the autoreactive potential of B cells by controlling BCR interactions (30).

In contrast, when the BCR class is changed by class switching and membrane-bound Igs are secreted as soluble Abs, the system may be exposed to an unpredicted pattern of autoreactivity induced just by the novel form of the Igs. This can be concluded from previous studies showing that substantial numbers of B cells are autoreactive when their BCR was tested as soluble Igs (4, 10). This points to an unexpected problem of regulating autoreactivity, as the Ig form expressed might be key for the specificity and affinity of Ag binding. Thus, seemingly harmless membrane-bound BCRs might uncover their autoreactivity after secretion as soluble Igs. As this form of autoimmunity is mediated by the Ig form, it seems to be unpredictable. In other words, it is conceivable that autoimmune reactions result from tolerant B cells whose secreted Ab is autoreactive despite an otherwise harmless membrane-bound BCR.

In this scenario, stimulation by an unknown Ag may activate m B cells to develop into memory B cells or plasma cells secreting potentially autoreactive Abs. The secreted Abs but not the membrane-bound BCR might recognize the unknown Ag with different affinity or specificity as compared with autoantigen. Accordingly, immune responses associated with chronic secretion of autoreactive Abs from otherwise tolerant B cells might be a major unnoticed cause of autoimmune diseases. Notably, this scenario differs from induction of autoimmune reactions by molecular mimicry, in which an Ag shares sequence or structural similarity with a self-antigen thereby leading to autoantibody production when encountering the Ag (31). In contrast, our data suggest that the potentially autoreactive Igs may not bind to autoantigen when expressed as BCR on the surface of B cells and that recognition of an unrelated Ag results in the secretion of autoreactive Abs. Because a substantial number of secreted Abs of peripheral B cells harbor autoreactive potential, it is currently unclear how such autoreactive Abs are prevented from damaging the body. Most likely, the protection relies on the $t_{1/2}$ of Abs, the duration of encountering the Ag, and regulatory functions of Igs, such as the binding to immune inhibitory receptors (32). In agreement with this, Abs possessing IgG4 isotype show increased stability and are often associated with autoimmune diseases (33). Altogether, this study suggests that characterization of the relationship between Ig form, Ag recognition, and B cell activation is required for understanding B cell selection and the development of autoimmune diseases.

analysis of GC178 IgG1 (top) and GC178gl IgG1 (bottom) Abs binding to OVA at indicated concentrations as shown in time versus resonance units (RU) plot. (**D**) Representative FACS analysis of GC178 IgM (left) and GC178gl IgM (right) BCRs on TKO cells for their OVA binding at 6, 4, and 2 μg/ml of OVA, compared with untransduced cells (control). (**E**) Top to bottom, representative analysis for calcium release of GC178 IgM (left column) and GC178gl IgM (right column) BCRs in response to 6, 4, and 2 μg/ml of OVA. (**F**) Same as in (D) for cOVA binding at 0.5, 0.25, and 0.05 μg/ml of cOVA. (**G**) Same as in (E) for GC178 IgM (left column) and GC178gl IgM (right column) calcium release in response to indicated concentrations of cOVA. The data in (B)–(G) are representative of a minimum of three independent experiments.

Acknowledgments

We thank F. Beckel for cell sorting and C. Ludwig for ELISA.

Disclosures

The authors have no financial conflicts of interest.

References

1. Davidson, A., and B. Diamond. 2001. Autoimmune diseases. *N. Engl. J. Med.* 345: 340–350.
2. Mietzner, B., M. Tsuiji, J. Scheid, K. Velinzon, T. Tiller, K. Abraham, J. B. Gonzalez, V. Pascual, D. Stichweh, H. Wardemann, and M. C. Nussenzweig. 2008. Autoreactive IgG memory antibodies in patients with systemic lupus erythematosus arise from nonreactive and polyreactive precursors. *Proc. Natl. Acad. Sci. USA* 105: 9727–9732.
3. Sherer, Y., A. Gorstein, M. J. Fritzler, and Y. Shoenfeld. 2004. Autoantibody explosion in systemic lupus erythematosus: more than 100 different antibodies found in SLE patients. *Semin. Arthritis Rheum.* 34: 501–537.
4. Wardemann, H., S. Yurasov, A. Schaefer, J. W. Young, E. Meffre, and M. C. Nussenzweig. 2003. Predominant autoantibody production by early human B cell precursors. *Science* 301: 1374–1377.
5. Halverson, R., R. M. Torres, and R. Pelanda. 2004. Receptor editing is the main mechanism of B cell tolerance toward membrane antigens. *Nat. Immunol.* 5: 645–650.
6. Nemazee, D. 2006. Receptor editing in lymphocyte development and central tolerance. *Nat. Rev. Immunol.* 6: 728–740.
7. Nemazee, D., and K. Buerki. 1989. Clonal deletion of autoreactive B lymphocytes in bone marrow chimeras. *Proc. Natl. Acad. Sci. USA* 86: 8039–8043.
8. Verkoczy, L., B. Duong, P. Skog, D. Aït-Azzouzene, K. Puri, J. L. Vela, and D. Nemazee. 2007. Basal B cell receptor-directed phosphatidylinositol 3-kinase signaling turns off RAGs and promotes B cell-positive selection. *J. Immunol.* 178: 6332–6341.
9. Hervé, M., K. Xu, Y. S. Ng, H. Wardemann, E. Albesiano, B. T. Messmer, N. Chiorazzi, and E. Meffre. 2005. Unmutated and mutated chronic lymphocytic leukemias derive from self-reactive B cell precursors despite expressing different antibody reactivity. *J. Clin. Invest.* 115: 1636–1643.
10. Tiller, T., M. Tsuiji, S. Yurasov, K. Velinzon, M. C. Nussenzweig, and H. Wardemann. 2007. Autoreactivity in human IgG+ memory B cells. *Immunity* 26: 205–213.
11. Yurasov, S., T. Tiller, M. Tsuiji, K. Velinzon, V. Pascual, H. Wardemann, and M. C. Nussenzweig. 2006. Persistent expression of autoantibodies in SLE patients in remission. *J. Exp. Med.* 203: 2255–2261.
12. Torres, M., R. May, M. D. Scharff, and A. Casadevall. 2005. Variable-region-identical antibodies differing in isotype demonstrate differences in fine specificity and idiotype. *J. Immunol.* 174: 2132–2142.
13. Tudor, D., H. Yu, J. Maupetit, A. S. Drillet, T. Bouceba, I. Schwartz-Cornil, L. Lopalco, P. Tuffery, and M. Bomsel. 2012. Isotype modulates epitope specificity, affinity, and antiviral activities of anti-HIV-1 human broadly neutralizing 2F5 antibody. *Proc. Natl. Acad. Sci. USA* 109: 12680–12685.
14. Maity, P. C., A. Blount, H. Jumaa, O. Ronneberger, B. F. Lillemeier, and M. Reth. 2015. B cell antigen receptors of the IgM and IgD classes are clustered in different protein islands that are altered during B cell activation. *Sci. Signal.* 8: ra93.
15. Übelhart, R., E. Hug, M. P. Bach, T. Wossning, M. Dühren-von Minden, A. H. Horn, D. Tsiantoulas, K. Kometani, T. Kurosaki, C. J. Binder, et al. 2015. Responsiveness of B cells is regulated by the hinge region of IgD. *Nat. Immunol.* 16: 534–543.
16. Tiller, T., C. E. Busse, and H. Wardemann. 2009. Cloning and expression of murine Ig genes from single B cells. *J. Immunol. Methods* 350: 183–193.
17. Tiller, T., E. Meffre, S. Yurasov, M. Tsuiji, M. C. Nussenzweig, and H. Wardemann. 2008. Efficient generation of monoclonal antibodies from single human B cells by single cell RT-PCR and expression vector cloning. *J. Immunol. Methods* 329: 112–124.
18. Köhler, F., E. Hug, C. Eschbach, S. Meixlsperger, E. Hobeika, J. Kofer, H. Wardemann, and H. Jumaa. 2008. Autoreactive B cell receptors mimic autonomous pre-B cell receptor signaling and induce proliferation of early B cells. *Immunity* 29: 912–921.
19. Bertinetti, C., F. Simon, K. Zirlik, K. Heining-Mikesch, D. Pfeifer, F. Osterroth, F. M. Rosenthal, and H. Veelken. 2006. Cloning of idiotype immunoglobulin genes in B cell lymphomas by anchored PCR and production of individual recombinant idiotype vaccines in *Escherichia coli*. *Eur. J. Haematol.* 77: 395–402.
20. Dühren-von Minden, M., R. Übelhart, D. Schneider, T. Wossning, M. P. Bach, M. Buchner, D. Hofmann, E. Surova, M. Follo, F. Köhler, et al. 2012. Chronic lymphocytic leukaemia is driven by antigen-independent cell-autonomous signalling. *Nature* 489: 309–312.
21. Meixlsperger, S., F. Köhler, T. Wossning, M. Reppel, M. Müschen, and H. Jumaa. 2007. Conventional light chains inhibit the autonomous signaling capacity of the B cell receptor. *Immunity* 26: 323–333.
22. Casadevall, A., and A. Janda. 2012. Immunoglobulin isotype influences affinity and specificity. *Proc. Natl. Acad. Sci. USA* 109: 12272–12273.
23. Tsuiji, M., S. Yurasov, K. Velinzon, S. Thomas, M. C. Nussenzweig, and H. Wardemann. 2006. A checkpoint for autoreactivity in human IgM+ memory B cell development. *J. Exp. Med.* 203: 393–400.
24. Burger, J. A., and N. Chiorazzi. 2013. B cell receptor signaling in chronic lymphocytic leukemia. *Trends Immunol.* 34: 592–601.
25. Lanemo Myhrinder, A., E. Hellqvist, E. Sidorova, A. Söderberg, H. Baxendale, C. Dahle, K. Willander, G. Tobin, E. Bäckman, O. Söderberg, et al. 2008. A new perspective: molecular motifs on oxidized LDL, apoptotic cells, and bacteria are targets for chronic lymphocytic leukemia antibodies. *Blood* 111: 3838–3848.
26. Sthoeger, Z. M., M. Wakai, D. B. Tse, V. P. Vinciguerra, S. L. Allen, D. R. Budman, S. M. Lichtman, P. Schulman, L. R. Weiselberg, and N. Chiorazzi. 1989. Production of autoantibodies by CD5-expressing B lymphocytes from patients with chronic lymphocytic leukemia. *J. Exp. Med.* 169: 255–268.
27. Sela-Culang, I., V. Kunik, and Y. Ofran. 2013. The structural basis of antibody-antigen recognition. *Front. Immunol.* 4: 302.
28. Pritsch, O., G. Hudry-Clergeon, M. Buckle, Y. Petillot, J. P. Bouvet, J. Gagnon, and G. Dighiero. 1996. Can immunoglobulin C(H)1 constant region domain modulate antigen binding affinity of antibodies? *J. Clin. Invest.* 98: 2235–2243.
29. Torres, M., and A. Casadevall. 2008. The immunoglobulin constant region contributes to affinity and specificity. *Trends Immunol.* 29: 91–97.
30. Kläsener, K., P. C. Maity, E. Hobeika, J. Yang, and M. Reth. 2014. B cell activation involves nanoscale receptor reorganizations and inside-out signaling by Syk. *Elife* 3: e02069.
31. Rose, N. R. 2015. Molecular mimicry and clonal deletion: a fresh look. *J. Theor. Biol.* 375: 71–76.
32. Ravetch, J. V., and L. L. Lanier. 2000. Immune inhibitory receptors. *Science* 290: 84–89.
33. Huijbers, M. G., J. J. Plomp, S. M. van der Maarel, and J. J. Verschuuren. 2018. IgG4-mediated autoimmune diseases: a niche of antibody-mediated disorders. *Ann. N. Y. Acad. Sci.* 1413: 92–103.